Inhibition of Endoplasmic Reticulum-Associated Degradation in CHO Cells Resistant to Cholera Toxin, *Pseudomonas aeruginosa* Exotoxin A, and Ricin

Ken Teter and Randall K. Holmes*

Department of Microbiology, University of Colorado Health Sciences Center, Denver, Colorado 80262

Many plant and bacterial toxins act upon cytosolic targets and must therefore penetrate a membrane barrier to function. One such class of toxins enters the cytosol after delivery to the endoplasmic reticulum (ER). These proteins, which include cholera toxin (CT), *Pseudomonas aeruginosa* exotoxin A (ETA), and ricin, move from the plasma membrane to the endosomes, pass through the Golgi apparatus, and travel to the ER. Translocation from the ER to the cytosol is hypothesized to involve the ER-associated degradation (ERAD) pathway. We developed a genetic strategy to assess the role of mammalian ERAD in toxin translocation. Populations of CHO cells were mutagenized and grown in the presence of two lethal toxins, ETA and ricin. Since these toxins bind to different surface receptors and attack distinct cytoplasmic targets, simultaneous acquisition of resistance to both would likely result from the disruption of a shared trafficking or translocation mechanism. Ten ETA- and ricin-resistant cell lines that displayed unselected resistance to CT and continued sensitivity to diphtheria toxin, which enters the cytosol directly from acidified endosomes, were screened for abnormalities in the processing of a known ERAD substrate, the Z form of α1-antitrypsin (α1AT-Z). Compared to the parental CHO cells, the rate of α1AT-Z degradation was decreased in two independent mutant cell lines. Both of these cell lines also exhibited, in comparison to the parental cells, decreased translocation and degradation of a recombinant CTA1 polypeptide. These findings demonstrated that decreased ERAD function was associated with increased cellular resistance to ER-translocating protein toxins in two independently derived mutant CHO cell lines.

Many plant and bacterial toxins exploit the eukaryotic secretory pathway in order to access the host cell cytoplasm (21, 26). Some proteins, such as diphtheria toxin (DT), enter cells by receptor-mediated endocytosis and pass directly from acidified endosomes to the cytoplasm. Others require additional trafficking and move from the endosomes to the Golgi en route to an exit site within the endoplasmic reticulum (ER). Toxins that follow the latter pathway bind to distinct surface receptors and attack a number of cytosolic targets: *Pseudomonas aeruginosa* exotoxin A (ETA), for example, binds to the α2-macroglobulin receptor and ADP ribosylates elongation factor 2; ricin adheres to the terminal galactose residues of glycolipids or glycoproteins and removes a specific adenine residue from the 28S rRNA; cholera toxin (CT) recognizes the ganglioside GM1 and ADP ribosylates Gsα; and Shiga toxin binds globoside Gb_3 and cleaves an adenine residue from the 28S rRNA in a manner similar to ricin. Each of these toxins has an AB structure that consists of a catalytic A moiety and a receptor-binding B moiety.

ER-translocating toxins follow distinct trafficking routes from the cell surface to the ER. CT endocytosis originates in caveolae and/or glycosphingolipid-enriched microdomains (28, 43), but the entry of ETA and Shiga toxin occurs through a clathrin-dependent mechanism (8, 33). In contrast, ricin is internalized by multiple endocytic pathways (34). Transport from the Golgi apparatus to the ER involves divergent pathways as well. Shiga toxin utilizes a rab 6-dependent route, while ETA and CT travel with the KDEL receptor along a separate, COPI-dependent path (9, 14, 22). Since these trafficking events precede translocation (31, 42), intoxication can be blocked by manipulations that slow or prevent retrograde transport to the ER (6, 9, 14, 19, 33, 36, 44).

Toxin resistance should also result from disruption of the ER translocation mechanism, but this process is not well understood. It has been proposed that the catalytic domain of an ER-translocating toxin is transferred to the cytosol by the ER-associated degradation (ERAD) pathway. This quality control system recognizes misfolded or misassembled proteins in the ER and exports them to the cytosol for ubiquitination and proteosomal degradation (4, 29, 32). Exposed hydrophobic residues in the catalytic domain of a partially unfolded toxin could thus trigger the ERAD mechanism and stimulate A moiety passage into the cytosol (12, 21). The cytosolic degradation that usually accompanies ERAD processing is presumably avoided, at least to some extent, because the A moieties of ER-translocating toxins display a codon bias for arginine over lysine (20) and hence are deficient in the target residues for ubiquitination.

Additional, albeit indirect, evidence for the ERAD toxin translocation model has been presented. Toxicity is impaired by alterations to a hydrophobic stretch within the ricin A domain (37) and by mutations that prevent unfolding of the ricin holotoxin (2). Yeast mutants harboring export-specific defects

* Corresponding author. Mailing address: Department of Microbiology, Box B-175, University of Colorado Health Sciences Center, 4200 East Ninth Ave., Denver, CO 80262. Phone: (303) 315-7903. Fax: (303) 315-6785. E-mail: Randall.Holmes@uchsc.edu.

in Sec61p, the major constituent of a "translocon" apparatus that directs both import and ERAD-mediated export of proteins across the ER membrane (32), cannot facilitate the ER-to-cytosol transfer of a ricin A chain fusion construct (38). CT, ETA, and ricin coimmunoprecipitate with Sec61p (16, 35, 42), while interaction with another ERAD component, protein disulfide isomerase, is a prerequisite for CT translocation (27, 41). Finally, the characteristics of ERAD-mediated proteolysis have been demonstrated for recombinant ricin and CT constructs (7, 40).

Despite a growing body of circumstantial evidence, the ERAD model of toxin translocation remains in question. Association with a specific ERAD factor, for example, does not necessarily correspond to a functional requirement for the ERAD system as a whole. Other uncertainties are due to the multiple proteolytic events involving ERAD: processing by this pathway can involve proteosome-dependent export from the ER, proteosome-independent export from the ER, ubiquitin-dependent export from the ER, ubiquitin-independent export from the ER, ubiquitin-dependent degradation, and ubiquitin-independent degradation (4, 29, 32). The ubiquitin-independent translocation of ricin and CT thus led one group to conclude that ricin translocation involved ERAD (38), while another group concluded that CT translocation was independent of ERAD function (35). An alternative, ERAD-independent translocation pathway has also been proposed for ETA (1). A functional requirement for ERAD in the ER-to-cytosol export of ricin, CT, and ETA would thus strengthen the evidence for the ERAD model of toxin translocation.

In this paper, we identified aberrant ERAD activity as a consequence of selection for toxin resistance in mammalian cultured cells. Toxin-resistant cell lines were isolated from a pool of mutagenized CHO cells grown in the presence of both ETA and ricin. These two lethal toxins bind different surface receptors and attack different cytosolic targets. Resistance to both should therefore occur much more frequently by altering a single function required for trafficking or translocation of both toxins than by altering two different functions, each of which is required for the action of only one of the toxins. To focus on translocation deficiencies, the resulting cell lines were screened for continued sensitivity to DT (which passes directly from acidified endosomes to the cytosol) and acquired resistance to CT. The varied endocytic and retrograde trafficking pathways followed by CT, ETA, and ricin should have further enhanced the selection of translocation mutants. We reasoned that, should ERAD function in the translocation of multiple toxins, some of the CT-, ETA-, and ricin-resistant cell lines might exhibit abnormal ERAD processing. This prediction was confirmed by monitoring the half-life of a known ERAD substrate, the Z variant of α1-antitrypsin (α1AT-Z), in the parental and mutant cell lines. Degradation of α1AT-Z was attenuated in two independent mutant cell lines. Impaired translocation and degradation of a recombinant CTA1 polypeptide was also observed in these two cell lines. Our work thus provides new genetic and functional evidence that decreased mammalian ERAD activity is associated with increased resistance to toxins such as CT, ETA, and ricin, most likely as a consequence of inhibited toxin translocation from the ER to the cytosol.

MATERIALS AND METHODS

Materials. Chemicals, ETA, and ricin were purchased from Sigma-Aldrich (St. Louis, Mo.). DT and CT were purified in our laboratory, as described previously (13, 25). The α1AT antibody was purchased from DAKO (Carpinteria, Calif.). Immobilized CTA (15) and α1AT antibodies were generated by incubating the antibodies with 100 mg of protein A-Sepharose overnight at 4°C in 1 ml of phosphate-buffered saline (PBS) supplemented with 0.1% bovine serum albumin. Tissue culture media and serum were purchased from Gibco BRL (Grand Island, N.Y.) or Mediatech (Herndon, Va.), while radiolabels were purchased from NEN Life Sciences (Boston, Mass.). A. McCracken (University of Nevada, Reno) kindly provided the pSV7/α1AT-Z plasmid (24).

Isolation of toxin-resistant cell lines. CHO cells bathed in Ham's F-12 medium supplemented with 10% fetal bovine serum were grown at 37°C and 5% CO_2 under humidified conditions. Cells grown to 80% confluency ($\sim 1.7 \times 10^7$ cells) in 10-cm-diameter dishes were mutagenized by exposing them for 24 h to 6 mM ethyl methanesulfonate. This treatment killed 50% of the exposed cells. The surviving cells were passaged to fresh 10-cm dishes at a 1:25 dilution and allowed to recover for 4 days. To screen for toxin resistance, the mutagenized cells were cultured in the presence of 100 ng of ricin per ml and 4.2 μg of ETA per ml for an additional 4 days. More than 99% of the cells died during this time. The remaining cells were washed and incubated with fresh medium in the absence of toxin until isolated colonies developed. Thirty to 60 colonies were observed on each of the eight dishes used in the screen, and 80 of the colonies were transferred to 96-well plates for subculture and confirmation of the selected phenotype. From the two dishes containing nonmutagenized cells, a total of 11 colonies were identified and cloned. Following transfer to the 96-well plate, each isolate was again subjected to a 4-day incubation with ricin and ETA. Only one of the nonmutagenized cell lines could be subcultured after this challenge; 21 of the 80 mutagenized cell lines also failed to survive this challenge.

Each remaining clone was expanded and screened for resistance to the morphological change (i.e., elongation) that is normally induced in CHO cells by treatment with CT (11). We found that 21 of the 60 clones (including 1 nonmutagenized clone) exhibited greater resistance to CT than the parental CHO cells from which they were derived. The CT-sensitive clones were discarded, and the CT-resistant cell lines were subcloned by limiting dilution to ensure the presence of pure clonal populations. The remaining nonmutagenized cell line ceased to grow during subculturing. Further analysis of the cloned and expanded mutant cell lines was performed as described below.

Quantitation of toxin resistance. Incorporation of [^{3}H]leucine into newly synthesized proteins was used to assess the effect of ETA, ricin, or DT on our parental and mutant CHO cell lines. Cells grown to 50 to 80% confluency in 24-well plates were exposed to ETA, ricin, or DT for 16 to 18 h, bathed with leucine-free medium for 30 min, and incubated for 1 h with 0.8 μCi of [^{3}H]leucine per ml in HEPES-buffered, leucine-free media. The medium and extracellular radiolabel were then removed and replaced with 10% trichloroacetic acid (TCA) in PBS for 1 h at 4°C. After a second 10-min wash with 10% TCA–PBS to remove TCA-soluble radiolabel, the cells were solubilized in 0.25 ml of 0.1 M KOH. The numbers of KOH-solubilized, TCA-precipitable cpm were determined by scintillation counting. Results from toxin-treated cells were expressed as a percentage of the values obtained from control cultures of the same cells incubated without toxin. Samples were run in triplicate, and the experiment was repeated at least twice for each cell line. The total numbers of cpm in the absence of toxin were consistently greater than 10,000 for all cell lines.

Intracellular cyclic AMP (cAMP) levels were determined in order to assess the effects of CT on our parental and mutant CHO cell lines. Cells grown to confluency in six-well plates were exposed to 10 ng of CT per ml for 2 h and then solubilized in 0.75 ml of acidic ethanol (1 N HCl–ethanol at a 1:100 ratio) for 15 min at 4°C. After a 10-min spin, the supernatant was collected, and the pellet was reextracted with 0.75 ml of an ice-cold ethanol-H_2O solution at 2:11 ratio. Supernatants from both extractions were combined and lyophilized overnight, while the remaining pellet was solubilized in 0.2 N NaOH for use in a Micro bicinchoninic acid (BCA) protein assay (Pierce, Rockford, Ill.). cAMP levels in the lyophilized cell extracts were quantitated with the Biotrak kit from Amersham-Pharmacia (Arlington Heights, Ill.) and were standardized as picomoles of cAMP per milligram of protein. Results were expressed as percentages of the values obtained with the CT-treated parental cells. Samples were run in duplicate, and each cell line, except clone 47, was tested at least twice.

Metabolic labeling and immunoprecipitation of α1AT-Z. Cells grown to near confluency in six-well plates were transiently transfected with pSV7/α1AT-Z by using the Lipofectamine reagent (Invitrogen, Carlsbad, Calif.) as per the manufacturer's instructions. At 48 h posttransfection, the cells were bathed in methionine-free medium for 1 h, incubated with 50 to 120 μCi of [^{35}S]methionine

per ml for 40 min, and returned to serum-free medium containing excess cold methionine. Cell extracts were collected immediately after pulse-labeling or after the indicated chase periods by solubilizing the monolayers in 1 ml of lysis buffer (25 mM Tris [pH 7.4], 20 mM NaCl, 1% deoxycholic acid, 1% Triton X-100, 1 mM phenylmethylsulfonyl fluoride [PMSF], 1 μg of pepstatin per ml, 1 μg of leupeptin per ml). After removal of insoluble debris by centrifugation, the cell extracts were mixed with immobilized α1AT antibodies for an overnight incubation. The bound material was then collected after multiple washes with 150 mM NaCl in NDET (1% NP-40, 0.4% deoxycholic acid, 5 mM EDTA, 10 mM Tris [pH 7.4]). Where indicated, the chase medium was also collected and subjected to α1AT immunoprecipitation. The immunoprecipitated proteins were electrophoresed on sodium dodecyl sulfate-polyacrylamide gel electrophoresis (SDS-PAGE) (9% polyacrylamide) gels, and PhosphoImager analysis (Bio-Rad; Hercules, Calif.) was used to visualize and quantitate α1AT-Z. Results for the chase intervals were expressed as percentages of the values obtained from the pulse-labeled cells and were derived from duplicate samples.

For α1AT-Z secretion assays, samples of medium were taken at specified intervals and replaced with fresh medium containing excess cold methionine. The values presented for these time course experiments were thus based on summation of the radioactivity from consecutive immunoprecipitations of secreted α1AT-Z. Secretion assay results were derived from duplicate samples and are expressed as a percentage of the values obtained from pulse-labeled cells. Other aspects of this protocol were identical to the description given above.

Metabolic labeling and immunoprecipitation of CTA1-CVIM. Cells transiently transfected with 1 μg of pcDNA3.1/CTA1-CVIM and 5 μl of Lipofectamine were metabolically labeled and processed as described above, with the following exceptions: cells were labeled with 150 μCi [35S]methionine/ml for 1 h, immunoprecipitations were with the immobilized anti-CTA B9 antibody, SDS-PAGE gels were run with 15% polyacrylamide, and single samples were used for each measurement. For the translocation assay, cells were solubilized at 4°C in 1% Triton X-114 containing 1 mM PMSF, 1 μg of pepstatin per ml, and 1 μg of leupeptin per ml. A centrifugal spin following warming of the cell extracts was performed in order to separate the Triton X-114 aqueous and detergent phases. The extent of translocation was calculated by expressing the detergent-phase value as a percentage of the combined values of the aqueous- and detergent-phase samples. Further details of the translocation and turnover assays are presented elsewhere (40).

RESULTS AND DISCUSSION

Quantitation of toxin resistance. ETA- and ricin-resistant CHO cell lines were generated as described in Materials and Methods. To measure the degree of toxin resistance, we incubated untreated and toxin-treated cells with 0.8 μCi of [3H]leucine per ml for 1 h at 37°C. Both ETA and ricin inhibit protein synthesis, so toxin activity can be assessed by comparing the amount of radiolabel incorporated into the newly synthesized proteins of untreated cells versus that in toxin-treated cells. Whereas 3 μg of ETA per ml decreased protein synthesis in the parental CHO cells to 4% of the control values without toxin, almost every mutant cell line was highly resistant to ETA at 3 μg/ml (Table 1). The increased resistance of the mutant cell lines to ricin was more variable and less dramatic, and no cell line was completely resistant to 100 ng of ricin per ml (Table 1). Whereas protein synthesis in the ricin-treated parental cells dropped to 11% of control levels, six mutants (clones 3, 6, 23, 24, 27, and 46) exhibited relatively high resistance, with protein synthesis levels greater than 70% of the untreated control values. Five mutant cell lines (clones 16, 18, 38, 47, and 54) showed intermediate resistance to ricin, with protein synthesis levels between 45 and 60% of the untreated control values. Five others (clones 4, 5, 34, 36, and 50) had slight resistance to ricin, with protein synthesis levels between 21 and 32% of the untreated control values. The four remaining mutants (clones 2, 7, 40, and 59) were not significantly more resistant to ricin than the parental cell line. In most cases,

TABLE 1. Toxin resistance in the parental and mutant cell lines

Cell line[a]	% Protein synthesis relative to untreated control cells[b]			% Parental cAMP response to 10 ng of CT/ml[c]
	3 μg of ETA/ml	100 ng of ricin/ml	1 ng of DT/ml	
Parental CHO Clones	4 ± 2	11 ± 6	54 ± 8	100
2	93 ± 6	20 ± 7	80 ± 5	53 ± 2
3*	94 ± 5	75 ± 4	48 ± 7	30 ± 3
4*	94 ± 7	21 ± 3	50 ± 6	47 ± 8
5*	93 ± 6	31 ± 1	62 ± 5	54 ± 7
6*	92 ± 2	74 ± 3	45 ± 10	17 ± 6
7	96 ± 4	17 ± 10	66 ± 6	66 ± 24
16*	96 ± 1	54 ± 11	52 ± 4	22 ± 0
18	76 ± 8	60 ± 7	75 ± 6	31 ± 10
23*	89 ± 4	74 ± 8	58 ± 4	31 ± 8
24*	86 ± 6	83 ± 1	56 ± 4	17 ± 3
27	95 ± 3	78 ± 5	66 ± 8	100 ± 24
34	61 ± 6	23 ± 5	60 ± 9	130 ± 8
36	80 ± 2	32 ± 4	78 ± 7	41 ± 1
38*	88 ± 6	48 ± 13	45 ± 0	58 ± 4
40	25 ± 3	18 ± 3	75 ± 6	85 ± 18
46*	96 ± 4	79 ± 9	53 ± 2	35 ± 13
47	90 ± 1	45 ± 4	81 ± 9	69
50*	90 ± 0	27 ± 9	64 ± 4	29 ± 1
54	51 ± 9	54 ± 3	57 ± 3	70 ± 14
59	102 ± 3	13 ± 2	63 ± 5	68 ± 23

[a] Clones marked with an asterisk exhibited the desired phenotype of cross-resistance to CT, ETA, and ricin with continued sensitivity to DT.

[b] Results obtained with ETA-, ricin-, or DT-treated cells are expressed as percentages of the control values from untreated cells and represent the averages ± standard deviations of two to three independent trials for each toxin.

[c] Results were standardized as picomoles of cAMP per milligram of protein and are expressed as percentages of the values obtained with parental cells, representing the averages ± standard deviations of two to three independent trials. Clone 47 was only tested once.

however, the clonal cell lines exhibited detectably increased resistance to both ETA and ricin.

The mutant cell lines were also screened for resistance to CT as a nonselected phenotype. This was initially determined during expansion of the cell lines with the use of a well-characterized morphological assay based on the CT-induced elongation of CHO cells (11). A second assay based on the CT-induced elevation of intracellular cAMP was performed with the final clones to confirm the results from the primary screen and to provide a quantitative assessment regarding the degree of CT resistance (Table 1). For each experiment, the cAMP concentration in the CT-treated parental cells was set at 100%, and the response of the mutant cell lines was expressed as a percentage of that control value. Basal cAMP levels in all cell lines were <100 pmol/mg of protein; this value rose to an average of 915 pmol/mg of protein (n = 11) in the parental cells after a 2-h incubation with 10 ng of CT/ml. All but three of the mutant clones were more resistant to CT than the parental CHO cells. Two cell lines (clones 6 and 24) were highly resistant to CT and had cAMP levels less than 20% of the control values. Six cell lines (clones 3, 16, 18, 23, 46, and 50) were moderately resistant to CT and had between 22 and 35% of the cAMP levels of the CT-treated parental cells. Five cell lines (clones 2, 4, 5, 36, and 38) were slightly resistant to CT and had between 41 and 58% of the cAMP levels of the CT-treated parental cells. The isolation of numerous cell lines with substantial levels of unselected resistance to CT suggested

that our strategy for disrupting a common toxin trafficking or translocation mechanism was successful.

Resistance to CT, ETA, and ricin could result from alterations of the endocytic pathway. Such defects could affect the action of toxins that pass directly from the endosomes to the cytosol as well as toxins that require endosome-to-Golgi transport. To test for this possibility, we screened our cell lines for resistance to DT, a toxin that enters the cytosol from acidified endosomes and inhibits protein synthesis by ADP ribosylation of elongation factor 2 (21, 26). As with ETA and ricin, DT activity was determined by comparing the extent of [³H]leucine incorporation into the newly synthesized proteins of untreated cells versus that in toxin-treated cells. A DT concentration of 1 ng/ml, which inhibited ~50% of protein synthesis in the parental CHO cells, was used in order to detect small changes in DT resistance for the mutant clones. Five cell lines (clones 2, 18, 36, 40, and 47) with increased resistance to DT (protein synthesis ≥ 75% of control levels) were identified with this assay.

Processing of ERAD substrate α1AT-Z. Resistance to CT, ETA, and ricin with continued sensitivity to DT was observed in 10 cell lines (clones 3, 4, 5, 6, 16, 23, 24, 38, 46, and 50). This phenotype could result from the disruption of a trafficking or translocation step common to CT, ETA, and ricin. The ERAD system might represent such a common step. We therefore tested these mutant cell lines for abnormalities in processing of the known ERAD substrate α1AT-Z. In wild-type cells, most of α1AT-Z is retained in the ER and eventually degraded by the ERAD mechanism, but some of the protein avoids degradation and is secreted into the extracellular medium (3, 17, 18). Analysis of α1AT-Z processing in our mutant cell lines could thus potentially identify alterations in degradation, secretion, or both. Furthermore, the turnover of α1AT-Z by both ubiquitin-dependent and ubiquitin-independent mechanisms (39) would allow us to detect disruptions in either of these ERAD pathways.

PhosphorImager quantitation of samples subjected to electrophoresis on SDS-PAGE gels was used to determine the amount of α1AT-Z immunoprecipitated from transiently transfected, metabolically labeled cells. Preliminary experiments in the parental CHO cells indicated that 50% of pulse-labeled α1AT-Z was lost from the intracellular pool between 1 and 2 h of chase and that ~20% of pulse-labeled α1AT-Z was secreted after 2 h of chase (Fig. 1). The material immunoprecipitated from each condition (pulse, chase, and chase medium) mainly consisted of a single protein with mobility of ~50 to 55 kDa. No corresponding band was isolated from mock-transfected cells (data not shown), and no other prominent bands were visualized with the procedure. Cellular processing of α1AT-Z accounts for the slightly different electrophoretic mobilities under each condition: the faster-migrating, ~50-kDa intracellular chase band represents an endoproteolytic intermediate (30) or deglycosylated (17) form of α1AT-Z, while additional glycosylation of the secreted protein (3, 17, 18) was responsible for its slower mobility. All samples ran at a slower mobility than the unglycosylated α1AT-Z isolated from pulse-labeled, tunicamycin-treated cells (data not shown).

We used a 2-h chase for initial screening of our mutant cell lines for alterations in the trafficking or degradation of
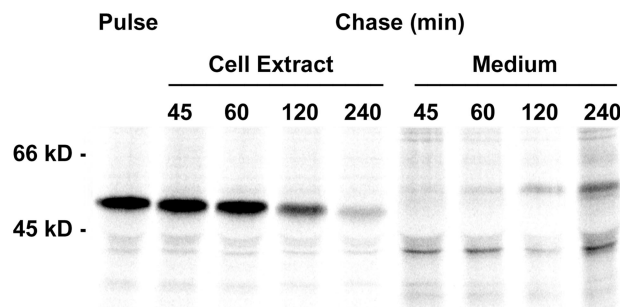

FIG. 1. Retention and secretion of α1AT-Z in the parental CHO cells. The processing of radiolabeled α1AT-Z was examined with the parental CHO cells. Transient expression of α1AT-Z was achieved by Lipofectamine transfection with the pSV7/α1AT-Z plasmid. At 48 h posttransfection, the cells were incubated in methionine-free medium for 1 h, exposed to 50 μCi of [³⁵S]methionine per ml for 40 min, and chased for the indicated times in the presence of excess cold methionine. Immunoprecipitates from both cell extracts and the extracellular medium were collected at each time interval and were visualized by SDS-PAGE with PhosphorImager scanning.

α1AT-Z (Table 2). After this interval, the parental cell line secreted ~20% of α1AT-Z, retained ~40% in an intracellular pool, and degraded ~40% of the protein. Only one mutant, clone 6, was indistinguishable from the parental cells by these criteria. The other mutant cell lines exhibited aberrant secretion and/or degradation of α1AT-Z. Clones 3, 4, and 50 degraded α1AT-Z normally, but secreted substantially less of the protein than the parental cells. Reduced secretion was also observed in three cell lines (clones 23, 24, and 38) that showed accelerated α1AT-Z degradation. One cell line, clone 5, displayed both decreased secretion and decreased degradation of α1AT-Z. Decreased degradation of α1AT-Z was also observed

TABLE 2. α1AT-Z processing in the parental and mutant cell lines

Class	Clone no.	% α1AT-Z[a]		
		Intracellular	Secreted	Degraded[b]
Parental CHO		40 ± 4	20 ± 3	42 ± 3
Mutant				
1	6	41 ± 3	22 ± 8	41 ± 7
2	3	51 ± 6	6 ± 2	44 ± 8
	4	50 ± 2	10 ± 4	41 ± 5
	50	45 ± 2	8 ± 4	46 ± 5
3	23	23 ± 6	5 ± 1	73 ± 6
	24	30 ± 2	10 ± 2	61 ± 0
	38	32 ± 6	13 ± 4	55 ± 9
4	5	65 ± 6	8 ± 2	29 ± 5
5	16	57 ± 1	18 ± 1	26 ± 1
	46	54 ± 6	26 ± 2	18 ± 4

[a] Results from a 2-h chase are expressed as percentages of the values obtained from pulse-labeled cells and represent the averages ± standard deviations of two to four independent experiments with duplicate samples.

[b] Percent degradation was determined by subtracting the combined values for the percentages of α1AT-Z in the cell extract (intracellular) and in the extracellular medium (secreted) from 100%.

in two cell lines (clones 16 and 46) that did not exhibit secretion deficiencies. The processing of α1AT-Z thus allowed us to divide the CT-, ETA-, and ricin-resistant cell lines into five general classes (Table 2): (i) no apparent ERAD or secretory abnormalities (class 1), (ii) normal ERAD activity with secretory defects (class 2), (iii) accelerated ERAD activity with secretory defects (class 3), (iv) decreased ERAD activity with secretory defects (class 4), and (v) decreased ERAD activity without secretory defects (class 5).

Toxin resistance in these cell lines could result from any mutation that prevents the catalytic moieties of ER-translocating toxins from accumulating in the cytosol. We hypothesized that the secretion-deficient class 2 mutants accomplished this by preventing toxin transport to the ER exit site, that the class 3 mutants with increased ERAD accomplished this by rapid proteosomal degradation of the cytosolic toxin, and that the class 4 and 5 mutants with decreased ERAD accomplished this by limiting toxin transfer from the ER to the cytosol. Each hypothesized result is based upon the available literature: (i) disruption of ER-to-Golgi and Golgi-to-ER transport renders cells resistant to multiple ER-translocating toxins (9, 14, 36, 44); (ii) toxin sensitization occurs after treatment with proteosomal inhibitors (42), so toxin resistance should result from increased ERAD and proteosomal activity; and (iii) ERAD inhibition often prevents substrate passage into the cytosol (4, 29, 32). The latter two predictions are based upon the hypothesized role of ERAD in toxin translocation. However, the accelerated turnover of α1AT-Z could also result from alterations to the proteosomal degradative pathway. Secretory defects in the class 3 and 4 mutants might complicate interpretation of the ERAD phenotype as well. We therefore focused our further attention on the class 5 mutants with attenuated ERAD and normal secretory function.

Toxin resistance in the class 5 mutant cell lines. Dose-response curves were generated to better characterize the toxin-resistant phenotype of clones 16 and 46. Both mutants were highly resistant to CT (Fig. 2A), highly resistant to ETA (Fig. 2B), and moderately resistant to ricin (Fig. 2C). Clones 16 and 46 were ~10-fold more resistant to ETA than the parental cells and displayed an ~3-fold increase in resistance to ricin. The degree of toxin resistance in these dose-response curves was somewhat less than that originally recorded in Table 1 and may reflect a partial loss of the toxin-resistant phenotype over time. Finally, the parental and mutant cell lines exhibited similar sensitivities to DT (Fig. 2D).

Kinetics of α1AT-Z processing in the class 5 mutant cell lines. We performed time course experiments to monitor the processing of α1AT-Z in the class 5 mutant cell lines (Fig. 3). As previously described, α1AT-Z was immunoprecipitated from transiently transfected, metabolically labeled cells. The pool of α1AT-Z remaining in the parental and mutant cell lines after chase intervals of 0, 45, 60, 120, and 240 min was then quantitated by SDS-PAGE and PhosphorImager analysis. Similar methods were used to determine the rate of α1AT-Z secretion from the class 5 mutants.

In the parental CHO cells, half of the intracellular pool of pulse-labeled α1AT-Z was lost to a combination of degradation and secretion between 1 and 2 h of chase. Secretion played a minor role in α1AT-Z processing during the first hour of chase, and significant degradation of the protein usually began
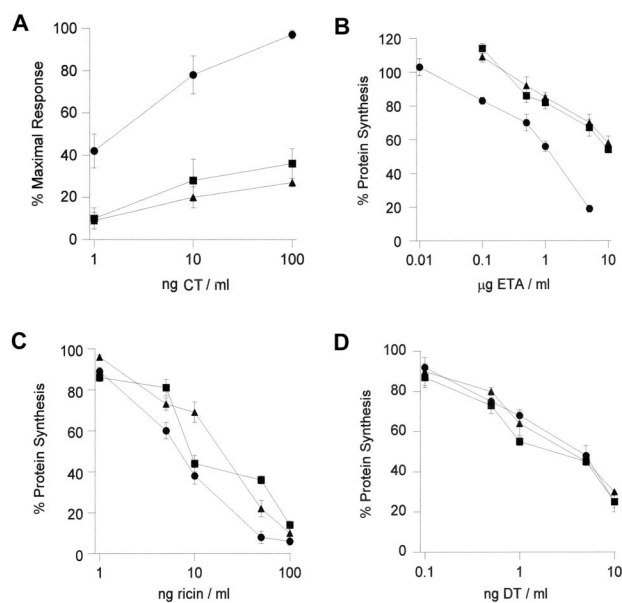

FIG. 2. Toxin dose-response curves for the parental and class 5 mutant cell lines. The extent of toxin resistance was determined for the class 5 mutants. (A) Clone 16 (triangles), clone 46 (squares), and the parental cells (circles) were incubated with various concentrations of CT for 2 h before intracellular cAMP levels were quantitated. Results were standardized as picomoles of cAMP per milligram of protein, are expressed as percentages of the maximal CT response, and represent the means ± standard errors of four independent experiments with triplicate samples. (B to D) Clone 16 (triangles), clone 46 (squares), and the parental cells (circles) were incubated with various concentrations of ETA (B), ricin (C), or DT (D) for 16 to 18 h before protein synthesis levels were measured. Results are expressed as percentages of the values from untreated control cells and represent the means ± standard errors of four to six independent experiments with triplicate samples.

after a 45-min lag (Fig. 3). These results were consistent with previous reports (3, 18). Decreased ERAD activity was detected in the class 5 mutants during the early stage of processing (Fig. 3A). Clones 16 and 46 degraded 10 to 20% less α1AT-Z than the parental cells after 45, 60, or 120 min of chase and exhibited a longer lag phase before the onset of α1AT-Z degradation. The relatively subtle inhibition of ERAD activity demonstrated with our cell lines was also observed in ERAD-deficient yeast mutants (5, 23) and suggested that ETA and ricin, the two toxins used in our initial selection strategy, exploit an ERAD mechanism that is required for cellular viability. Nevertheless, the observed inhibition of ERAD was sufficient to alter the intracellular half-life of α1AT-Z: the parental cell line retained 50% of pulse-labeled α1AT-Z after 1.7 h of chase, whereas 50% of the intracellular protein remained after an extended 2.4 h of chase in clones 16 and 46. Neither clone displayed significant alterations to α1AT-Z secretion (Fig. 3B). Resistance to multiple ER-translocating toxins thus correlated with inhibition of ERAD activity against α1AT-Z.

Translocation and degradation of CTA1-CVIM in the class 5 mutant cell lines. Inefficient degradation and an extended substrate half-life often result from the inhibition of ERAD-mediated export to the cytosol. By extension, then, CT resis-
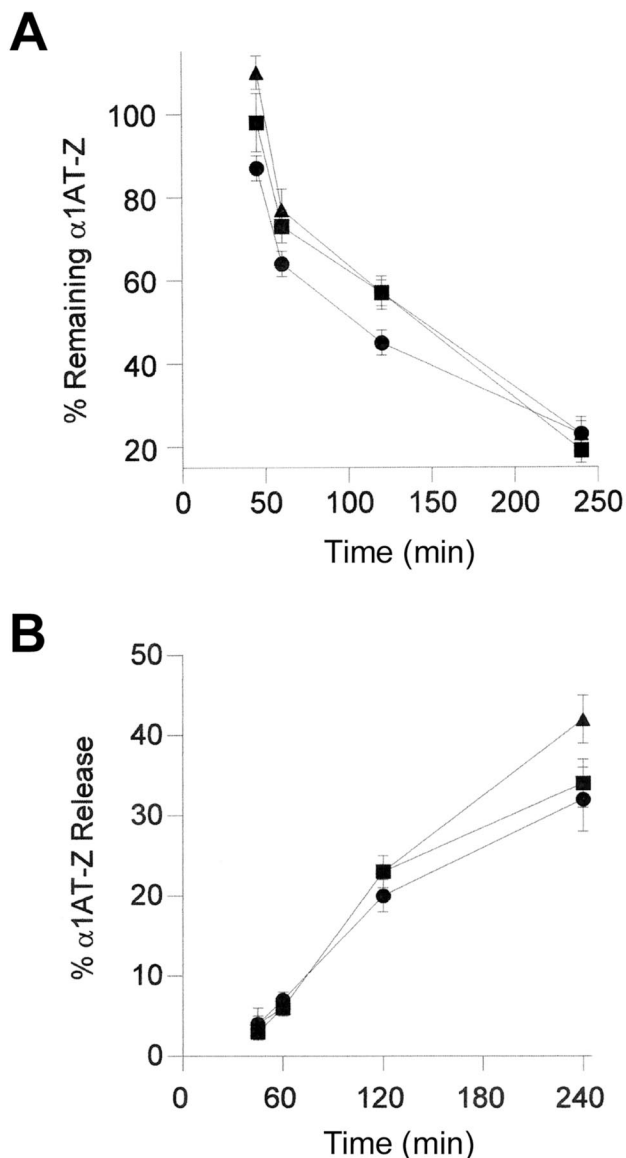
A

B

FIG. 3. Processing of α1AT-Z in the parental and class 5 mutant cell lines. The degradation (A) and secretion (B) of ERAD substrate α1AT-Z were monitored in clone 16 (triangles), clone 46 (squares), and the parental CHO cells (circles). Pulse-chase experiments with transiently transfected, metabolically labeled cells were performed as described in the legend to Fig. 1. The results are expressed as percentages of the pulse-labeled values and represent the means ± standard errors of at least four independent experiments with duplicate samples.
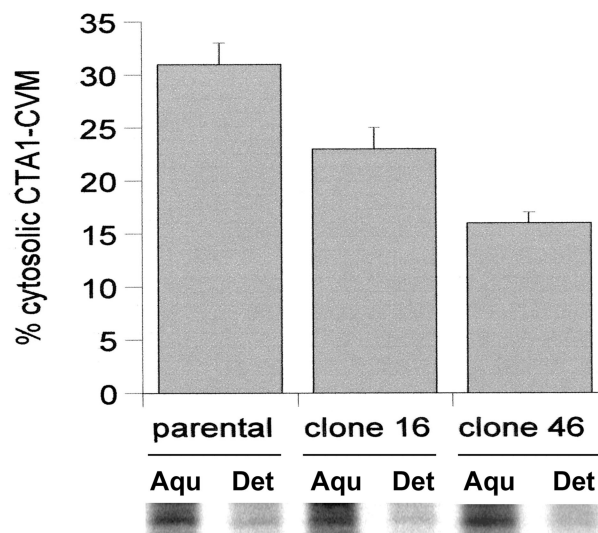

FIG. 4. Translocation of CTA1-CVIM in the parental and class 5 mutant cell lines from the ER to the cytosol. Cells transfected with CTA1-CVIM were incubated with 150 μCi of [^{35}S]methionine per ml for 1 h and were then solubilized in ice-cold Triton X-114. After warming to 37°C, aqueous (i.e., ER lumen) and detergent (i.e., cytosolic) phases of the cell extracts were separated by centrifugation. Both phases were subjected to anti-CTA immunoprecipitation, and SDS-PAGE with PhosphorImager analysis was used to visualize and quantitate the immunoisolated material. The cytosolic pools of CTA1-CVIM are expressed as percentages of the total CTA1-CVIM found in both aqueous (Aqu.)- and detergent (Det.)-phase samples. Results represent the means ± standard errors of at least four independent experiments for each cell line.

tance in clones 16 and 46 could have resulted from a defective translocation mechanism that limited access of the catalytic CTA1 polypeptide to the cytosol. We tested this prediction directly by monitoring the translocation of CTA1-CVIM, a recombinant tagged form of the CTA1 polypeptide (Fig. 4). CTA1-CVIM was expressed from the pcDNA3.1 eukaryotic expression vector and consisted of the native CTA leader sequence, the catalytic domain of an inactive CTA1 variant, and a C-terminal CVIM farnesylation motif. A separate report demonstrated that this construct, when transiently transfected into CHO cells, was inserted into the ER lumen and then transferred to the cytosol for proteosomal degradation. Entry into the cytosol was monitored by the appearance of CTA1-CVIM in the detergent phase of a cell extract generated with Triton X-114; this property of detergent-phase partitioning resulted from the cytosolic addition of a 15-carbon fatty acid farnesyl moiety to CTA1-CVIM. A variant construct in which the CVIM farnesylation motif was replaced by a nonfunctional SVIM motif always remained in the aqueous phase of the Triton X-114 cell extracts (40).

Clone 16, clone 46, and the parental CHO cells were transiently transfected with CTA1-CVIM, incubated for 1 h with 150 μCi of [^{35}S]methionine per ml, and solubilized at 4°C in Triton X-114. The aqueous and detergent phases of the Triton X-114 lysates were separated with a short centrifugal spin after warming to 37°C. Anti-CTA immunoprecipitates from both aqueous and detergent phases were then visualized and quantitated by SDS-PAGE with PhosphorImager analysis. We found that 31% of CTA1-CVIM segregated into the detergent (i.e., cytosolic) phase of Triton X-114 cell extracts generated from the parental CHO cells. In contrast, 22% of radiolabeled CTA1-CVIM was detected in the detergent phase of Triton X-114 cell extracts generated from clone 16, and 15% of radiolabeled CTA1-CVIM was detected in the detergent phase of Triton X-114 cell extracts generated from clone 46 (Fig. 4).
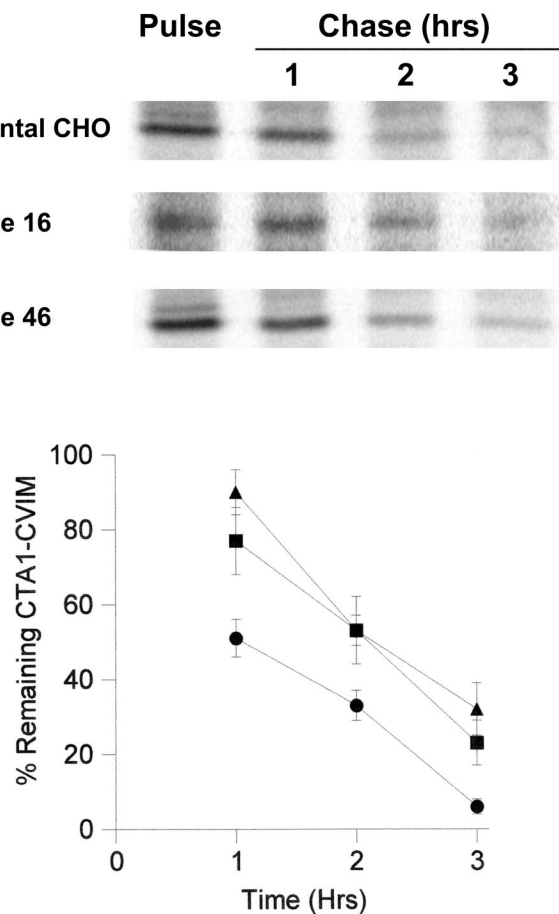
FIG. 5. Degradation of CTA1-CVIM in the parental and class 5 mutant cell lines. The turnover of CTA1-CVIM was monitored in clone 16 (triangles), clone 46 (squares), and the parental CHO cells (circles). Cells transfected with CTA1-CVIM were incubated with 150 μCi of [^{35}S]methionine per ml for 1 h and were then chased in serum-free medium containing an excess of cold methionine. Anti-CTA immunoprecipitates collected from cell extracts generated with Triton X-100 at the indicated time points were visualized and quantitated by SDS-PAGE with PhosphorImager analysis. The results are expressed as percentages of the pulse-labeled values and represent the means ± standard errors of at least four independent experiments for each cell line.

CTA1 translocation was therefore inhibited in both clones 16 and 46: the extent of CTA1-CVIM translocation that had occurred by the end of the 1-h labeling period was 30% less in clone 16 and 50% less in clone 46 than in the parental CHO cells. ERAD inhibition in clones 16 and 46 thus correlated with the decreased movement of CTA1-CVIM from the ER to the cytosol in these mutant cell lines.

Because ERAD substrates are degraded in the cytosol, we predicted that the decreased translocation activity in clones 16 and 46 would correspond to an increased half-life for CTA1-CVIM. The data presented in Fig. 5 supported this prediction. Pulse-chase experiments to monitor the turnover of CTA1-CVIM demonstrated that the 1.0-h half-life of CTA1-CVIM in

the parental cells was extended to 2.1 to 2.2 h in clones 16 and 46. We concluded that clones 16 and 46 did not efficiently degrade CTA1-CVIM because the mutant clones did not efficiently export CTA1-CVIM from the ER lumen to the cytosolic site of degradation. Collectively, then, our work strongly suggested that toxin resistance in clones 16 and 46 resulted from an ERAD-mediated defect in toxin export from the ER to the cytosol.

Proteosomal degradation of cytosolic substrates. Attenuated degradation of α1AT-Z and CTA1-CVIM was unlikely to result from a direct effect on the proteosome, as proteosomal inhibition does not prevent toxin entry into the cytosol (40) and leads to toxin sensitization rather than toxin resistance (42). To confirm that proteosomal activity was unaltered in clones 16 and 46, we used an established assay (10) to monitor the turnover of short-lived cytosolic proteins in the parental and the class 5 mutant cell lines. The ratio of TCA-soluble cpm to total cpm derived from cells pulse-labeled with [^{3}H]leucine demonstrated that clone 16, clone 46, and the parental cells each degraded 10% of the labeled proteins after 1 h of chase ($n = 2$). Thus, attenuated degradation of α1AT-Z and CTA1-CVIM in clones 16 and 46 could not be attributed to decreased proteosomal activity.

Conclusion. In summary, we have identified reduced ERAD activity in a subset of CHO mutant cell lines that were selected for simultaneous resistance to ETA and ricin and also exhibited an unselected increase in resistance to CT. Toxin resistance was also correlated with decreased translocation of CTA1-CVIM. It is unlikely that the selection of ETA- and ricin-resistant cell lines would generate defects in two unrelated ER dislocation mechanisms, one utilized by the ERAD substrate α1AT-Z and the other utilized by CTA1. Our findings thus provide presumptive functional evidence for the role of mammalian ERAD in the passage of multiple ER-translocating toxins into the cytosol, although the exact biochemical explanations for ERAD dysfunction in our mutant cell lines remain to be identified. The mutant cell lines described in this study should serve as valuable tools for the continuing investigation of how ERAD activity modulates toxin translocation into the cytosol.

REFERENCES

1. **Alami, M., M. P. Taupiac, H. Reggio, A. Bienvenue, and B. Beaumelle.** 1998. Involvement of ATP-dependent *Pseudomonas* exotoxin translocation from a late recycling compartment in lymphocyte intoxication procedure. Mol. Biol. Cell **9:**387–402.
2. **Argent, R. H., L. M. Roberts, R. Wales, J. D. Robertus, and J. M. Lord.** 1994. Introduction of a disulfide bond into ricin A chain decreases the cytotoxicity of the ricin holotoxin. J. Biol. Chem. **269:**26705–26710.
3. **Brodbeck, R. M., and J. L. Brown.** 1992. Secretion of alpha-1-proteinase inhibitor requires an almost full length molecule. J. Biol. Chem. **267:**294–297.
4. **Brodsky, J. L., and A. A. McCracken.** 1999. ER protein quality control and proteasome-mediated protein degradation. Semin. Cell Dev. Biol. **10:**507–513.
5. **Brodsky, J. L., E. D. Werner, M. E. Dubas, J. L. Goeckeler, K. B. Kruse, and A. A. McCracken.** 1999. The requirement for molecular chaperones during endoplasmic reticulum-associated protein degradation demonstrates that

protein export and import are mechanistically distinct. J. Biol. Chem. **274:** 3453–3460.

6. **Chaudhary, V. K., Y. Jinno, D. FitzGerald, and I. Pastan.** 1990. *Pseudomonas* exotoxin contains a specific sequence at the carboxyl terminus that is required for cytotoxicity. Proc. Natl. Acad. Sci. USA **87:**308–312.

7. **Di Cola, A., L. Frigerio, J. M. Lord, A. Ceriotti, and L. M. Roberts.** 2001. Ricin A chain without its partner B chain is degraded after retrotranslocation from the endoplasmic reticulum to the cytosol in plant cells. Proc. Natl. Acad. Sci. USA **98:**14726–14731.

8. **FitzGerald, D., R. E. Morris, and C. B. Saelinger.** 1980. Receptor-mediated internalization of *Pseudomonas* toxin by mouse fibroblasts. Cell **21:**867–873.

9. **Girod, A., B. Storrie, J. C. Simpson, L. Johannes, B. Goud, L. M. Roberts, J. M. Lord, T. Nilsson, and R. Pepperkok.** 1999. Evidence for a COP-I-independent transport route from the Golgi complex to the endoplasmic reticulum. Nat. Cell Biol. **1:**423–430.

10. **Gronostajski, R. M., A. B. Pardee, and A. L. Goldberg.** 1985. The ATP dependence of the degradation of short- and long-lived proteins in growing fibroblasts. J. Biol. Chem. **260:**3344–3349.

11. **Guerrant, R. L., L. L. Brunton, T. C. Schnaitman, L. I. Rebhun, and A. G. Gilman.** 1974. Cyclic adenosine monophosphate and alteration of Chinese hamster ovary cell morphology: a rapid, sensitive in vitro assay for the enterotoxins of *Vibrio cholerae* and *Escherichia coli.* Infect. Immun. **10:**320–327.

12. **Hazes, B., and R. J. Read.** 1997. Accumulating evidence suggests that several AB-toxins subvert the endoplasmic reticulum-associated protein degradation pathway to enter target cells. Biochemistry **36:**11051–11054.

13. **Holmes, R. K., and R. B. Perlow.** 1975. Quantitative assay of diphtherial toxin and of immunologically cross-reacting proteins by reversed passive hemagglutination. Infect. Immun. **12:**1392–1400.

14. **Jackson, M. E., J. C. Simpson, A. Girod, R. Pepperkok, L. M. Roberts, and J. M. Lord.** 1999. The KDEL retrieval system is exploited by *Pseudomonas* exotoxin A, but not by Shiga-like toxin-1, during retrograde transport from the Golgi complex to the endoplasmic reticulum. J. Cell Sci. **112:**467–475.

15. **Jobling, M. G., and R. K. Holmes.** 2001. Biological and biochemical characterization of variant A subunits of cholera toxin constructed by site-directed mutagenesis. J. Bacteriol. **183:**4024–4032.

16. **Koopmann, J. O., J. Albring, E. Huter, N. Bulbuc, P. Spee, J. Neefjes, G. J. Hammerling, and F. Momburg.** 2000. Export of antigenic peptides from the endoplasmic reticulum intersects with retrograde protein translocation through the Sec61p channel. Immunity **13:**117–127.

17. **Le, A., G. A. Ferrell, D. S. Dishon, Q. Q. Le, and R. N. Sifers.** 1992. Soluble aggregates of the human PiZ alpha 1-antitrypsin variant are degraded within the endoplasmic reticulum by a mechanism sensitive to inhibitors of protein synthesis. J. Biol. Chem. **267:**1072–1080.

18. **Le, A., K. S. Graham, and R. N. Sifers.** 1990. Intracellular degradation of the transport-impaired human PiZ alpha 1-antitrypsin variant. Biochemical mapping of the degradative event among compartments of the secretory pathway. J. Biol. Chem. **265:**14001–14007.

19. **Lencer, W. I., C. Constable, S. Moe, M. G. Jobling, H. M. Webb, S. Ruston, J. L. Madara, T. R. Hirst, and R. K. Holmes.** 1995. Targeting of cholera toxin and *Escherichia coli* heat labile toxin in polarized epithelia: role of COOH-terminal KDEL. J. Cell Biol. **131:**951–962.

20. **London, E., and C. L. Luongo.** 1989. Domain-specific bias in arginine/lysine usage by protein toxins. Biochem. Biophys. Res. Commun. **160:**333–339.

21. **Lord, J. M., and L. M. Roberts.** 1998. Toxin entry: retrograde transport through the secretory pathway. J. Cell Biol. **140:**733–736.

22. **Majoul, I., K. Sohn, F. T. Wieland, R. Pepperkok, M. Pizza, J. Hillemann, and H. D. Soling.** 1998. KDEL receptor (Erd2p)-mediated retrograde transport of the cholera toxin A subunit from the Golgi involves COPI, p23, and the COOH terminus of Erd2p. J. Cell Biol. **143:**601–612.

23. **McCracken, A. A., I. V. Karpichev, J. E. Ernaga, E. D. Werner, A. G. Dillin, and W. E. Courchesne.** 1996. Yeast mutants deficient in ER-associated degradation of the Z variant of alpha-1-protease inhibitor. Genetics **144:**1355–1362.

24. **McCracken, A. A., K. B. Kruse, and J. L. Brown.** 1989. Molecular basis for defective secretion of the Z variant of human alpha-1-proteinase inhibitor: secretion of variants having altered potential for salt bridge formation between amino acids 290 and 342. Mol. Cell. Biol. **9:**1406–1414.

25. **Mekalanos, J. J., R. J. Collier, and W. R. Romig.** 1978. Purification of cholera toxin and its subunits: new methods of preparation and the use of hypertoxinogenic mutants. Infect. Immun. **20:**552–558.

26. **Olsnes, S., J. Wesche, and P. O. Falnes.** 1999. Binding, uptake, routing and translocation of toxins with intracellular sites of action, p. 73–93. *In* J. E. Alouf and J. H. Freer (ed.), The comprehensive sourcebook of bacterial protein toxins, 2nd ed. Academic Press, San Diego, Calif.

27. **Orlandi, P. A.** 1997. Protein-disulfide isomerase-mediated reduction of the A subunit of cholera toxin in a human intestinal cell line. J. Biol. Chem. **272:**4591–4599.

28. **Orlandi, P. A., and P. H. Fishman.** 1998. Filipin-dependent inhibition of cholera toxin: evidence for toxin internalization and activation through caveolae-like domains. J. Cell Biol. **141:**905–915.

29. **Perlmutter, D. H.** 1999. Misfolded proteins in the endoplasmic reticulum. Lab. Investig. **79:**623–638.

30. **Qu, D., J. H. Teckman, S. Omura, and D. H. Perlmutter.** 1996. Degradation of a mutant secretory protein, alpha1-antitrypsin Z, in the endoplasmic reticulum requires proteasome activity. J. Biol. Chem. **271:**22791–22795.

31. **Rapak, A., P. O. Falnes, and S. Olsnes.** 1997. Retrograde transport of mutant ricin to the endoplasmic reticulum with subsequent translocation to cytosol. Proc. Natl. Acad. Sci. USA **94:**3783–3788.

32. **Romisch, K.** 1999. Surfing the Sec61 channel: bidirectional protein translocation across the ER membrane. J. Cell Sci. **112:**4185–4191.

33. **Sandvig, K., S. Olsnes, J. E. Brown, O. W. Petersen, and B. van Deurs.** 1989. Endocytosis from coated pits of Shiga toxin: a glycolipid-binding protein from *Shigella dysenteriae* 1. J. Cell Biol. **108:**1331–1343.

34. **Sandvig, K., and B. van Deurs.** 1999. Endocytosis and intracellular transport of ricin: recent discoveries. FEBS Lett. **452:**67–70.

35. **Schmitz, A., H. Herrgen, A. Winkeler, and V. Herzog.** 2000. Cholera toxin is exported from microsomes by the Sec61p complex. J. Cell Biol. **148:**1203–1212.

36. **Simpson, J. C., C. Dascher, L. M. Roberts, J. M. Lord, and W. E. Balch.** 1995. Ricin cytotoxicity is sensitive to recycling between the endoplasmic reticulum and the Golgi complex. J. Biol. Chem. **270:**20078–20083.

37. **Simpson, J. C., J. M. Lord, and L. M. Roberts.** 1995. Point mutations in the hydrophobic C-terminal region of ricin A chain indicate that Pro250 plays a key role in membrane translocation. Eur. J. Biochem. **232:**458–463.

38. **Simpson, J. C., L. M. Roberts, K. Romisch, J. Davey, D. H. Wolf, and J. M. Lord.** 1999. Ricin A chain utilises the endoplasmic reticulum-associated protein degradation pathway to enter the cytosol of yeast. FEBS Lett. **459:**80–84.

39. **Teckman, J. H., R. Gilmore, and D. H. Perlmutter.** 2000. Role of ubiquitin in proteasomal degradation of mutant alpha(1)-antitrypsin Z in the endoplasmic reticulum. Am. J. Physiol. Gastrointest. Liver Physiol. **278:**G39–G48.

40. **Teter, K., R. L. Allyn, M. G. Jobling, and R. K. Holmes.** 2002. Transfer of the cholera toxin A1 polypeptide from the endoplasmic reticulum to the cytosol is a rapid process facilitated by the endoplasmic reticulum-associated degradation pathway. Infect. Immun. **70:**6166–6171.

41. **Tsai, B., C. Rodighiero, W. I. Lencer, and T. A. Rapoport.** 2001. Protein disulfide isomerase acts as a redox-dependent chaperone to unfold cholera toxin. Cell **104:**937–948.

42. **Wesche, J., A. Rapak, and S. Olsnes.** 1999. Dependence of ricin toxicity on translocation of the toxin A-chain from the endoplasmic reticulum to the cytosol. J. Biol. Chem. **274:**34443–34449.

43. **Wolf, A. A., M. G. Jobling, S. Wimer-Mackin, M. Ferguson-Maltzman, J. L. Madara, R. K. Holmes, and W. I. Lencer.** 1998. Ganglioside structure dictates signal transduction by cholera toxin and association with caveolae-like membrane domains in polarized epithelia. J. Cell Biol. **141:**917–927.

44. **Yoshida, T., C. C. Chen, M. S. Zhang, and H. C. Wu.** 1991. Disruption of the Golgi apparatus by brefeldin A inhibits the cytotoxicity of ricin, modeccin, and *Pseudomonas* toxin. Exp. Cell Res. **192:**389–395.